Molecular Crystals and Liquid Crystals

ISSN: 1542-1406 (Print) 1563-5287 (Online) Journal homepage: http://www.tandfonline.com/loi/gmcl20

# XRD, FTIR, $^{1}$H NMR, $^{13}$C NMR and UV spectroscopic and computational studies of [3-(hydroxyimino)butan-2-ylidene]furan-2'-carbohydrazide

**Pelin Kurnaz, Cigdem Yuksektepe Ataol, Humeyra Bati & Orhan Buyukgungor**

**To cite this article:** Pelin Kurnaz, Cigdem Yuksektepe Ataol, Humeyra Bati & Orhan Buyukgungor (2016) XRD, FTIR, $^{1}$H NMR, $^{13}$C NMR and UV spectroscopic and computational studies of [3-(hydroxyimino)butan-2-ylidene]furan-2'-carbohydrazide, Molecular Crystals and Liquid Crystals, 634:1, 61-72, DOI: 10.1080/15421406.2016.1177904

**To link to this article:** http://dx.doi.org/10.1080/15421406.2016.1177904

MOLECULAR CRYSTALS AND LIQUID CRYSTALS
2016, VOL. 634, 61–72
http://dx.doi.org/10.1080/15421406.2016.1177904

Taylor & Francis
Taylor & Francis Group

# XRD, FTIR, $^{1}$H NMR, $^{13}$C NMR and UV spectroscopic and computational studies of [3-(hydroxyimino)butan-2-ylidene]furan-2′-carbohydrazide

Pelin Kurnaz[a], Cigdem Yuksektepe Ataol[b], Humeyra Bati[a], and Orhan Buyukgungor[c]

[a]Department of Chemistry, Faculty Art and Sciences, Ondokuz Mayis University, Samsun, Turkey; [b]Department of Physics, Faculty of Science, Cankiri Karatekin University, Uuyazi, Cankiri, Turkey; [c]Department of Physics, Faculty Art and Sciences, Ondokuz Mayis University, Samsun, Turkey

**ABSTRACT**

[3-(hydroxyimino)butan-2-ylidene]furan-2′-carbohydrazide (1) has been synthesized and characterized by IR, 1H NMR, 13C NMR, UV/vis and X-ray diffraction. In addition to the experimental studies, the optimized structure, vibrational parameters, chemical shifts, thermodynamic properties, ionization energy, electron affinity, electronegativity, global chemical hardness and chemical softness of the molecule have been investigated by using DFT with B3LYP/6.311G(d, p) and PBEPBE/6.311G(d, p) basis sets. HOMO and LUMO energies were calculated by TD-DFT approach in two different solvents. The experimental results of the compound have been compared with theoretical results and it is found to show good agreement with calculated values.

**KEYWORDS**

Single crystal; Hydrazone; Furan; Oxime; DFT; Energy gap

## 1. Introduction

Oximes and hydrazones are the two important classes of compounds owing to their wide applications in industry, medicine, detection and determination of various metal ions [1].

Hydrazones are used as intermediates in synthesis [2], as functional groups in metal carbonyls [3], in organic compounds [4, 5] and in particular in hydrazone Schiff base ligands [6–9], which are among others employed in dinuclear catalysts [10]. Furthermore, hydrazones exhibit physiological activities in the treatment of several diseases such as tuberculosis. This activity is attributed to the formation of stable chelate complexes with transition metals that catalyze physiological processes [11–13]. They also act as herbicides, insecticides, nematocides, rodenticides, plant growth regulators, sterilants for houseflies, among other applications [11, 12, 14]. In analytical chemistry, hydrazones find applications as multidentate ligands for transition metals in colorimetric or fluorimetric determinations [15, 16]. Hydrazones and their metal complexes show varied applications in the field such as antifungal, antibacterial, antitumoral activity, antioxidative, cytotoxic studies [17–19] and its derivates are used as fungicides and in the treatment of diseases such as tuberculosis, leprosy and mental disorders

**CONTACT** Cigdem Yuksektepe Ataol yuksektepe.c@karatekin.edu.tr, yuksekc85@gmail.com Department of Physics, Faculty of Science, Cankiri Karatekin University, 18100 Uluyazi, Cankiri, Turkey.
Color versions of one or more of the figures in the article can be found online at www.tandfonline.com/gmcl.
Supplementary data for this article can be accessed on the publisher's website

[20]. The coordination chemistry, biochemistry and of hydrazones have attracted increasing interest due to their chelating ability and pharmacological applications [21]. Furoic acid hydrazide and their metal complexes are of resent interest [18].

Oximes are becoming increasingly important as analytical, biochemical and antimicrobial reagents and they have received attention due to their use as liquid crystal and dyes [22]. The vast literature on structural studies of oxime complexes reveals some interesting features of its coordinative behavior [23]. Diacetyl monoxime and its various derivaties are extensively used as biologically active complexing agents and analytical regents [24]. There is interest in the coordination chemistry of oximes as they have served as models for biological systems such as vitamin B12 and as myocardial perfusion imaging agents [25].

Furan derivative is an important class of heterocyclic compound that possesses important biological properties. From last few decades, a considerable amount of attention has been focused on the synthesis of furan derivatives and screening them for different pharmacological activities. The furan ring system is the basic skeleton of numerous compounds possessing cardiovascular activities. An iodinated lipophilic furan derivative is widely used in the treatment of ventricular and atrial fibrillation. These moieties are widely employed as antibacterial, antiviral, anti-inflammatory, antifungal, antitumor, antihyperglycemic, analgesic, anticonvulsant, etc. Slight change in substitution pattern in furan nucleus causes distinguishable difference in their biological activities [26].

Schiff bases have played an important role in the development coordination chemistry and Schiff bases ligands are well known for their wide range of application in pharmaceutical and industrial fields [22, 27]. The coordination compounds derived from Schiff bases with transition metals have been studied with wide scope of their applications [28].

In this work, we report the experimental and the theoretical studies of single crystal structure ($C_9H_{11}N_3O_3$) and also, in the following we discuss IR, NMR, UV spectra of compound by using Density Functional Theory (DFT) calculations. The calculated results by all these methods were compared with the experimental results.

## 2. Experimental

### 2.1. General

The electronic absorption spectra of title compound were recorded at room temperature in methanol/acetonitrile (5/3) solution (the concentration is $10^{-3}$ M) on a Unicam UV2 UV–VIS spectrometer working between 200 and 900 nm. IR spectrum was recorded on a JASCO FT/IR-430 spectrophotometer using KBr pellets. $^1$H NMR spectra were obtained by using a Bruker Avance-III 400 MHz spectrometer in DMSO-$d_6$, at 298 K. The elemental analysis was recorded on Thermo Flash 2000 Elemental Analyser.

### 2.2. Synthesis of the title compound

The compound was synthesized as shown in Scheme 1 by the following procedure. Preparation of the ligand $LH_2$: 2-furoic acid hydrazide (0.04 g, 0.3 mmol) was dissolved in anhydrous ethanol (10 ml). To this solution was added dropwise diacetylmonoxime (0.03 g, 0.3 mmol) in anhydrous ethanol (10 ml). The mixture was refluxed for 3 h and after cooling for 4 days, white crystalline compound was separated out. Yield (50%). The formula, melting point and (C, H, N)'s elemental analysis results have been given in Table 1.

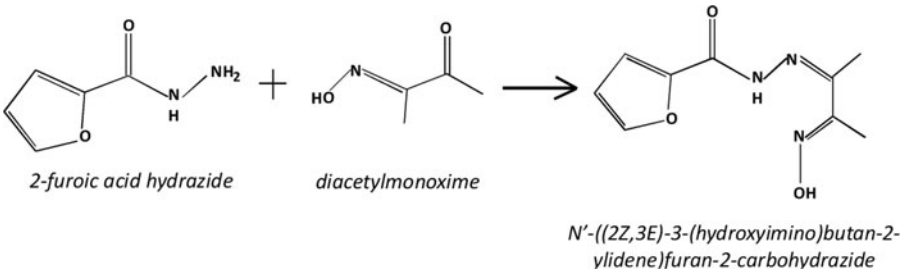


**Scheme 1.** The synthesis of the target compound.

### 2.3. Single crystal XRD

The data collection was performed at 296 K on a Stoe-IPDS-2 image plate detector using a graphite monochromated Mo-$K_\alpha$ radiation ($\lambda = 0.71073$ Å). Data collection and cell refinement were performed using X-AREA [29] and X-RED32 [29]. The structure was solved by direct methods using SHELXS-97 [30] and refined by a full-matrix least-square procedure using the program SHELXL-2013 [31]. Molecular graphics were performed using ORTEP-3 [32]. All non-hydrogen atoms were easily found from the difference Fourier map and refined anisotropically. The all hydrogen atoms were included using a riding model and refined isotropically with CH = 0.93 Å (for furan ring), $CH_3$ = 0.96 Å, NH = 0.86 Å and OH = 0.82 Å $U_{iso}(H) = 1.2\ U_{eq}$ (1.5 for methyl group). The H atoms of the C9 methyl group are disordered. Crystals of **(1)** were found approximately 0.5:0.5 ratio to be twinned. The crystal was a non-morehedral twin crystal with two reciprocal lattice differently oriented giving rise to double diffraction spot sets. Reflection data were measured for the two twin domains, scaled and combined together, but overlapping reflections could not be satisfactorily measured and were discarded, leading to a data completeness of about 76%.

Relevant crystal data and details of the structure determinations are given in Table 2.

### 2.4. Computational methodology

The molecular structures of the title compound in the ground state (in vacuo) were optimized by DFT methods to include correlation corrections with the 6–311G(d, p) basis set and two different basis functions. In DFT calculations, hybrid functionals are also used, including the Becke's three-parameter functional (B3) [33], which defines the exchange functional as the linear combination of Hartree-Fock, local, and gradient-corrected exchange terms. The B3 hybrid functional was used in combination with the correlation functionals of Lee et al. [34].

Then vibrational frequencies for optimized molecular structures have been calculated. The geometry of the title compounds, together with that of tetramethylsilane (TMS) is fully optimized. $^1$H NMR chemical shifts are calculated within GIAO approach [35, 36] applying B3LYP and PBEPBE method with 6–311G(d, p) basis set. The isotropic shielding values were

**Table 1.** Elemental analysis results of **(1)**.

| Ligand $LH_2$ | Melting point (°C) | MA (g/mol) | Color | Calculated/Found% | | |
|---|---|---|---|---|---|---|
| $C_9H_{11}N_3O_2$ | 255* | 209.20 | White | C | H | N |
| | | | | 51.67<br>51.89 | 5.30<br>5.25 | 20.09<br>19.27 |

**Table 2.** Crystallographic data of **(1)**.

| Empirical formula | $C_9H_{11}N_3O_3$ |
|---|---|
| Molecular weight | 209.21 |
| Temperature, $T$ (K) | 296 |
| Wavelength (Å) | 0.71073 |
| Crystal system | Triclinic |
| Crystal size ($mm^3$) | 0.020 × 0.150 × 0.280 |
| Space group | $P$-1 |
| $a$ (Å) | 7.1568(8) |
| $b$ (Å) | 7.6648(9) |
| $c$ (Å) | 9.7394(11) |
| $\alpha$ (°) | 79.424(9) |
| $\beta$ (°) | 68.514(9) |
| $\gamma$ (°) | 83.273(9) |
| Volume, $V$ ($Å^3$) | 487.96(10) |
| $Z$ | 2 |
| Calculated density (Mg $m^{-3}$) | 1.424 |
| $\theta$ Range (°) | 3.06–25.65 |
| Index ranges | $h = -7 \rightarrow 7, k = -8 \rightarrow 9, l = -11 \rightarrow 11$ |
| Measured reflections | 5424 |
| Independent reflections | 1305 |
| Observed reflections ($I > 2\sigma$) | 601 |
| Goodness of fit on $F^2$ | 0.816 |
| $R_1$ indice ($I > 2\sigma$) | 0.0435 |
| $wR_2$ indice ($I > 2\sigma$) | 0.0700 |
| $\Delta\rho_{min}$, $\Delta\rho_{max}$ (e $Å^{-3}$) | −0.349, 0.428 |

used to calculate the isotropic chemical shifts $\delta$ with respect to TMS. $\delta_{iso}(X) = \sigma_{TMS}(X) - \sigma_{iso}(X)$, where $\delta_{iso}$ is isotropic chemical shift and $\sigma_{iso}$ is isotropic shielding.

UV–Visible spectra, electronic transitions, vertical excitation energies and oscillator strengths were computed with the time dependent (TD) DFT method. Besides these, the lowest unoccupied molecular orbital (LUMO) and highest occupied molecular orbital (HOMO) energy differences for these species were calculated with this method. All the calculations were performed using the Gaussview molecular visualization program [37] and Gaussian 03 program on a personal computer [38].

In addition, thermodynamic properties, ionization potential, electron affinity, electronegativity, global chemical hardness and chemical softness of the molecule have been investigated by using DFT with B3LYP/6–311G(d, p) and PBEPBE/6–311G(d, p) basis sets.

## 3. Results and discussion

### 3.1. Description of the crystal structure using XRD

The asymmetric unit of the title compound **(1)** is shown in Fig. 1(a). The compound **(1)** contains furan ring, hydrazone and oxime groups. An examination of the deviations from the least-square planes shows that the furan ring A(O1-C1), B(C1/C5/N1/N2/C6) and C(C6/C8/N3/O3) are nearly planar with maximum deviations for the C1 [0.0024 (15) Å], N1 [-0.0540 (17) Å] and N3 [−0.0148 (10) Å] atoms, respectively. The selected bond lengths, dihedral and torsion angles are shown in Table 3. All bond lengths and angles are within the normal ranges.

One of the compound's groups, the oxime (−C=N−OH) groups possess stronger hydrogen bonding capabilities than alcohols, phenols and carboxylic acids. The hydrogen-bond systems in the crystals of oximes have been analyzed and a correlation between a pattern of hydrogen

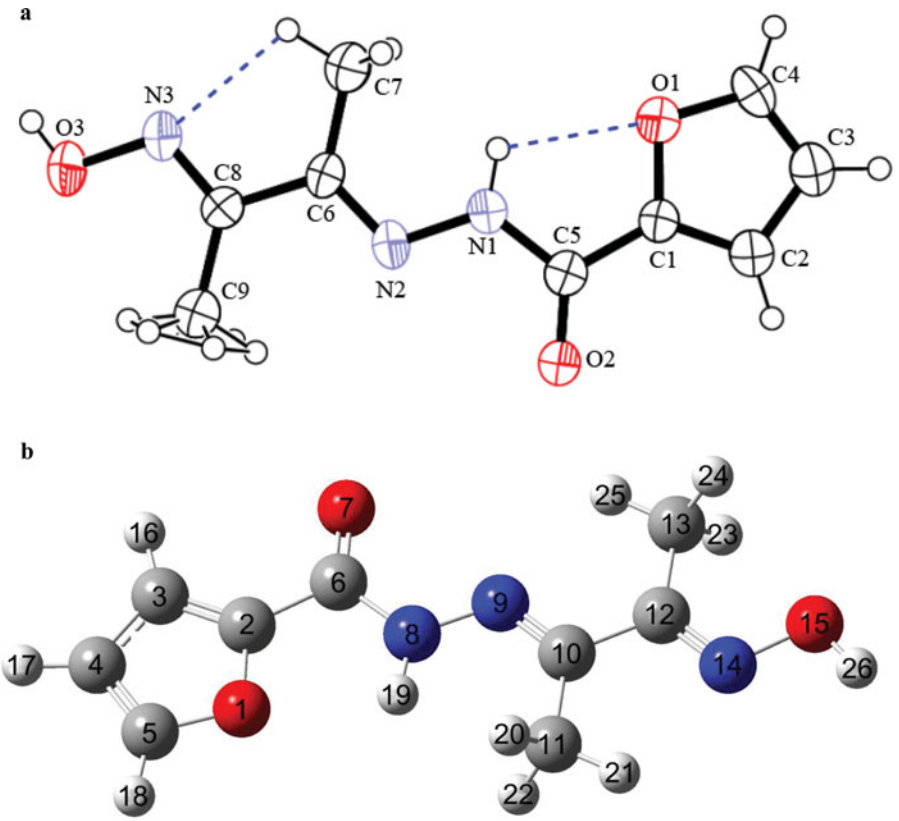


**Figure 1.** (a) ORTEP drawing of the basic crystallographic unit, showing the atom-numbering scheme. Displacement ellipsoids are drawn at the 30% probability level and H atoms are shown as small spheres of arbitrary radii. Intra-molecular hydrogen bonds are shown such as N1-H1 …O1 and C7-H7C …N3. (b) Gaussview drawing of the molecular structure.

bonding and N-O bond lengths has been suggested. The configurational and/or conformational isomers of glyoxime derivatives (dioximes) have also been analyzed [39]. The torsion angles of the oxime (O3-N3=C8-C6) and the hydrazone (C5-N1=N2-C6) units are 177.6(3)° and 175.4(3)°. These results are in good agreement with related literature [40]. The N1–N2 bond distance of 1.383(3) Å is appreciably shorter than a typical N–N single bond, such as that found in free 2,4-dinitrophenylhydrazone, 1.405(6) Å [41]; this suggests the existence of a delocalized double bond. The N3=C8 and N2=C6 distances of 1.290(3) Å and 1.296(3) Å, respectively, are typical of a double bond. The C=N and N–O distances of the free oximes are close to those commonly found in oxime derivatives [C=N = 1.292(13) Å and N–O = 1.396(3) Å] [42].

The crystal structure has six intra-intermolecular hydrogen bonds (Table 4). Intramolecular hydrogen bonds are shown in Fig. 1(a). Intramolecular hydrogen bonds (C-H …N and N-H …O) in the molecule are formed S(5) graph set motifs (see Fig. 1(a)). As can be seen from Fig. 2, the intermolecular hydrogen bonds are highly effective in forming the polymeric chains. Fig. 2(a) shows that the intermolecular interactions occur between O3 atom of the oxime group (as donor) with O2 atom of the carbonyl group (as acceptor) and C2, C3 and C4 atoms of the furan rings (as donor) with N3, O3 atoms of the oxime groups (as acceptor) and O2 atom of the carbonyl group (as acceptor), respectively. C2-H2 …N3 and O3-H3A …O2 intermolecular hydrogen bonds linked two different molecules together resulting

**Table 3.** Selected geometrical parameters of the title compound **(1)** with X-ray structure and DFT method.

| | Experimental | B3LYP 6–311G(d, p) | PBEPBE 6–311G(d, p) |
|---|---|---|---|
| Bond lengths (Å) | | | |
| N3–O3 | 1.406(3) | 1.397 | 1.403 |
| N1–N2 | 1.383(3) | 1.351 | 1.348 |
| C5–O2 | 1.222(4) | 1.211 | 1.223 |
| C1–O1 | 1.366(3) | 1.374 | 1.382 |
| C5–N1 | 1.362(4) | 1.389 | 1.399 |
| C6–N2 | 1.296(3) | 1.289 | 1.305 |
| C8–N3 | 1.290(3) | 1.287 | 1.303 |
| C1–C5 | 1.458(4) | 1.476 | 1.476 |
| C6–C8 | 1.476(4) | 1.478 | 1.471 |
| Bond angles (°) | | | |
| N1–N2–C6 | 114.3(3) | 118.4 | 117.8 |
| C8–N3–O3 | 112.3(2) | 111.7 | 111.1 |
| C5–N1–N2 | 122.6(3) | 120.1 | 120.3 |
| O1–C1–C5 | 119.0(3) | 119.7 | 119.9 |
| N2–C6–C8 | 115.5(3) | 115.6 | 115.5 |
| C6–C8–N3 | 113.2(3) | 115.7 | 115.5 |
| O2–C5–N1 | 124.1(3) | 124.9 | 124.7 |
| C1–C5–N1 | 112.5(3) | 113.3 | 113.3 |
| C1–O1–C4 | 106.5(2) | 106.9 | 106.7 |
| Torsion angles (°) | | | |
| O1–C1–C5-O2 | 178.4(4) | 180.0 | −180.0 |
| C5–C1–O1-C4 | − 178.4(3) | −180.0 | 180.0 |
| C1–C5–N1-N2 | 175.4(3) | 180.0 | 180.0 |
| C5–N1–N2-C6 | − 178.8(3) | 180.0 | −180.0 |
| N1–N2–C6-C8 | 175.3(3) | −180.0 | 180.0 |
| N2–C6–C8-N3 | − 172.6(3) | −180.0 | −180.0 |
| C6–C8–N3-O3 | 177.6(3) | −180.0 | −180.0 |

in an $R_2^2(8)$ hydrogen bonding motif. C4-H4 …O2, C3-H3 …O3 and O3-H3A …O2 bonds linked three different molecules together resulting in an $R_2^3(7)$ hydrogen bonding motif while C2-H2 …N3, C4-H4 …O2 and C3-H3 …O3 bonds linked three different molecules together resulting in an $R_3^3(22)$ hydrogen bonding motif. As a result, these intermolecular interactions repeat each other *c*-direction in the crystal lattice (see Fig. 2(b)).

## 3.2. Theoretical studies using DFT method

### 3.2.1. Optimized structure

Fig. 1(b) shows the optimized structure of the single crystal. The optimized molecular geometries are calculated by using B3LYP/6–311G(d, p) and PBEPBE/6–311G(d, p) methods. Some selected geometric parameters experimentally obtained and theoretically calculated by B3LYP/6–311G(d, p) and PBEPBE/6–311G(d, p) methods are listed in Table 3 and compared with X-ray results. It is well known that DFT optimized geometric parameters are usually in

**Table 4.** Hydrogen bond interactions of the title compound **(1)** (Å, °).

| Hydrogen bond (Å,°) | D–H | H …A | D …A | D–H …A |
|---|---|---|---|---|
| N1-H1 …O1 | 0.86 | 2.23 | 2.643(4) | 109 |
| C7-H7C …N3 | 0.96 | 2.28 | 2.738(4) | 109 |
| O3–H3A …O2$^{i}$ | 0.82 | 2.00 | 2.809(3) | 171 |
| C2-H2 …N3$^{ii}$ | 0.93 | 2.41 | 3.318(4) | 164 |
| C4-H4 …O2$^{iii}$ | 0.93 | 2.42 | 3.170(4) | 138 |
| C3-H3 …O3$^{iv}$ | 0.93 | 2.50 | 3.386(4) | 159 |

Symmetry codes: (i): *x*, *y*, −1+*z*; (ii): *x*, *y*, 1+*z*; (iii): *x*, 1+*y*, *z*; (iv): *x*, 1+*y*, 1+*z*.

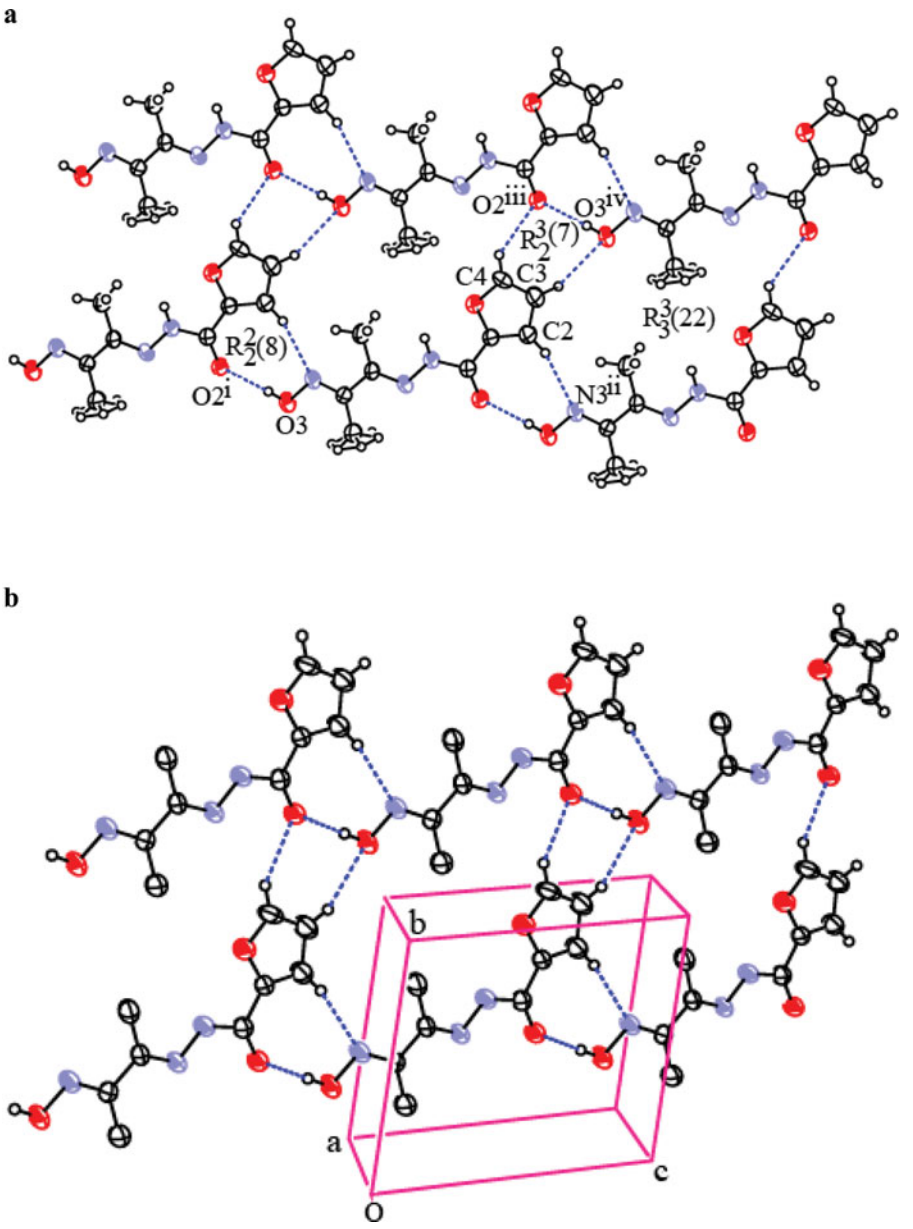


**Figure 2.** (a) A diagram showing the O3–H3A …O2$^{i}$, C2-H2 …N3$^{ii}$, C4-H4 …O2$^{iii}$ and C3-H3 …O3$^{iv}$ intermolecular hydrogen bonds and rings in the title compound. (b) Showing intermolecular hydrogen bonds of the crystal structure and rings in the unit cell. Only those H atoms involved in the hydrogen bonding interactions are shown. [Symmetry code: (i) : *x*, *y*, −1+ *z*; (ii): *x*, *y*, 1 + *z*; (iii): *x*, 1 + *y*, *z*; (iv): *x*, 1 + *y*, 1 + *z*].

good agreement with experimental values and more accurate than Hartree-Fock and semi-empirical methods, due to inclusion of electron correlation. The largest differences between experimental and calculated bond lengths, bond angles and torsion angles are about 0.032 Å and 0.037 Å, 4.1° and 3.5°, 7.4° and 7.4° for B3LYP/6–311G(d, p) and PBEPBE/6–311G(d, p), respectively. The optimized bond lengths provided by B3LYP/6-311G(d, p) method are the closest to the experimental values while the optimized dihedral angles provided by PBEPBE/6-311G(d, p) method are the closest to the experimental values (see Table 3).

### 3.2.2. Vibrational spectra

The experimental IR spectrum of the ligand $LH_2$ shows several bands in 4000–450 $cm^{-1}$ region (Fig. 3).

The functional groups of the compound **(1)** have been identified from the infrared spectrum. In the IR spectrum of compound **(1)**, characteristic bands are observed at 1763/1663 $cm^{-1}$, 1662 $cm^{-1}$, 1596 $cm^{-1}$ assigned to the $\upsilon$(C=O), $\upsilon$(C=N) and $\upsilon$(C=N) hydrazone vibrations, respectively. The stretching vibration $\upsilon$(OH) is higher than the stretching vibration $\upsilon$(NH) in literature. In this paper, because of intermolecular hydrogen bonds, the stretching vibration $\upsilon$(OH) is much lower than the stretching vibration $\upsilon$(NH). The experimental $\upsilon$(OH) and $\upsilon$(NH) stretching modes are observed at 3263 $cm^{-1}$ and 3384 $cm^{-1}$. The value of the stretching vibrational frequency of the oxime group is compared with the other oxime groups in literature [43]. A strong band at 1087/1040 $cm^{-1}$ in the spectrum of **(1)** is mainly attributed to $\upsilon$(N–O) vibration. The medium intensity band at 1184 $cm^{-1}$ is ascribed to $\upsilon$(N–N) vibration.

The other stretching, bending, twist, rocking, scissoring modes and calculated vibrational frequencies can be seen in S1.

### 3.2.3. NMR spectra

The $^1$H NMR spectrum of the ligand showed peaks corresponding to (NH) proton at 10.54 ppm. The characteristic oxime OH proton is observed at 11.63 ppm. These chemical shifts are characteristic values for hydrazones and oximes [23]. The furan ring protons appear at 7.95, 7.38 and 6.71–6.70 ppm. The $CH_3$ protons neighboring on oxime groups ($CH_3$-C=NOH) and imine group ($CH_3$-C=N-NH) appear at 2.50 and 2.15–2.09 ppm, respectively. These data are in agreement with previously reported for similar compounds [23].

In the $^{13}$C NMR spectrum of ligand, different signals, which were observed at 146.53 ppm (-C=N-NH), 155.02 ppm (–C=NOH) and 164.37 ppm (–C=O), show asymmetrically hydrazone and oxime locations [23]. The signals of the C furan ring were observed at 112 ppm. The signals of $CH_3$ were shown at 9.92 and 12.04 ppm. The detailed theoretical and experimental $^{13}$C NMR and $^1$H NMR spectral data are given in S2.

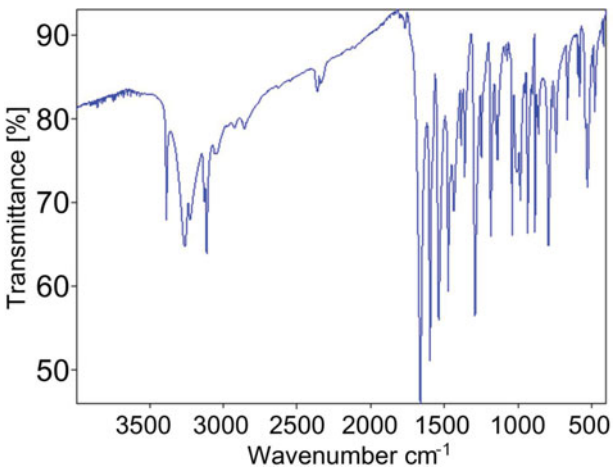


**Figure 3.** Experimental FT-IR spectrum of the title compound.

**Table 5.** The calculated absorption wavelength (λ), excitation energies (*E*), oscillator strength (*f*) and frontier orbital energies of compound **(1)** by TD-DFT method.

| Methods | λ (nm) | *E* (ev) | *f* | $E_{HOMO}$ (ev) | $E_{LUMO}$ (ev) | $E_{HOMO-1}$ (ev) | $E_{LUMO+1}$ (ev) |
|---|---|---|---|---|---|---|---|
| | Methanol | | | −6.404 | −1.896 | −6.977 | −0.802 |
| B3LYP 6–311G(d, p) | 300.38 | 4.1276 | 0.8994 | | | | |
| | 266.27 | 4.6564 | 0.0006 | | | | |
| | 262.40 | 4.7249 | 0.0052 | | | | |
| | Acetonitrile | | | −6.404 | −1.897 | −6.977 | −0.863 |
| | 300.62 | 4.1242 | 0.9033 | | | | |
| | 266.22 | 4.6573 | 0.0006 | | | | |
| | 262.48 | 4.7235 | 0.0525 | | | | |
| PBEPBE | Methanol | | | −5.455 | −2.608 | −6.106 | −1.665 |
| | 359.53 | 3.4485 | 0.6441 | | | | |
| 6–311G(d, p) | 325.91 | 3.8043 | 0.0511 | | | | |
| | 322.74 | 3.8416 | 0.0003 | | | | |
| | Acetonitrile | | | −5.456 | −2.608 | −6.107 | −1.665 |
| | 359.98 | 3.4459 | 0.6488 | | | | |
| | 325.98 | 3.8034 | 0.0506 | | | | |
| | 322.67 | 3.8424 | 0.0003 | | | | |
| Experimental | 236 | | | | | | |
| | 310 | | | | | | |

### 3.2.4. Electronic absorption spectra

The excited states were taken into account for the TD-DFT method based on the B3LYP/6–311G(d, p) and PBEPBE/6–311G(d, p) levels including two different solvents (acetonitrile and methanol) in order to investigate the properties of electronic absorption. The energies of four important molecular orbitals of the title compound **(1)**: the second highest and highest occupied MO's (HOMO and HOMO –1), the lowest and the second lowest unoccupied MO's (LUMO and LUMO +1) were calculated and are presented in Table 5.

The calculations were also performed with methanol and acetonitrile solvents in order to investigate the effect of MO transitions. The energy gap between HOMO and LUMO is a critical parameter in determining molecular electrical transport properties [43]. The experimental UV-Vis absorption spectrum is shown in Fig. 4. Experimentally, electronic absorption spectrum of the title compound in methanol/acetonitrile (5/3) solution shows two bands at 310 and 236 nm. One of the absorption bands at 310 nm is caused by the n $\rightarrow \pi*$ transition and the other band at 236 nm is due to $\pi \rightarrow \pi*$ transition. The $\pi \rightarrow \pi*$ transitions are expected to occur relatively at lower wavelength, due to the consequence of the extended aromaticity of the furan ring. Then the n $\rightarrow \pi*$ transition is more significant due to the presence of lone pair of electrons in the oxygen and nitrogen atoms in the molecular structure. Some frontier molecular orbitals are shown in Fig. 5. The energy gap of HOMO-LUMO explains the eventual charge

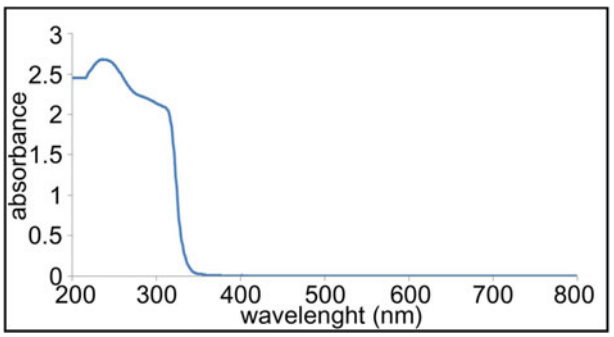


**Figure 4.** The experimental UV-Vis spectrum of the title compound.

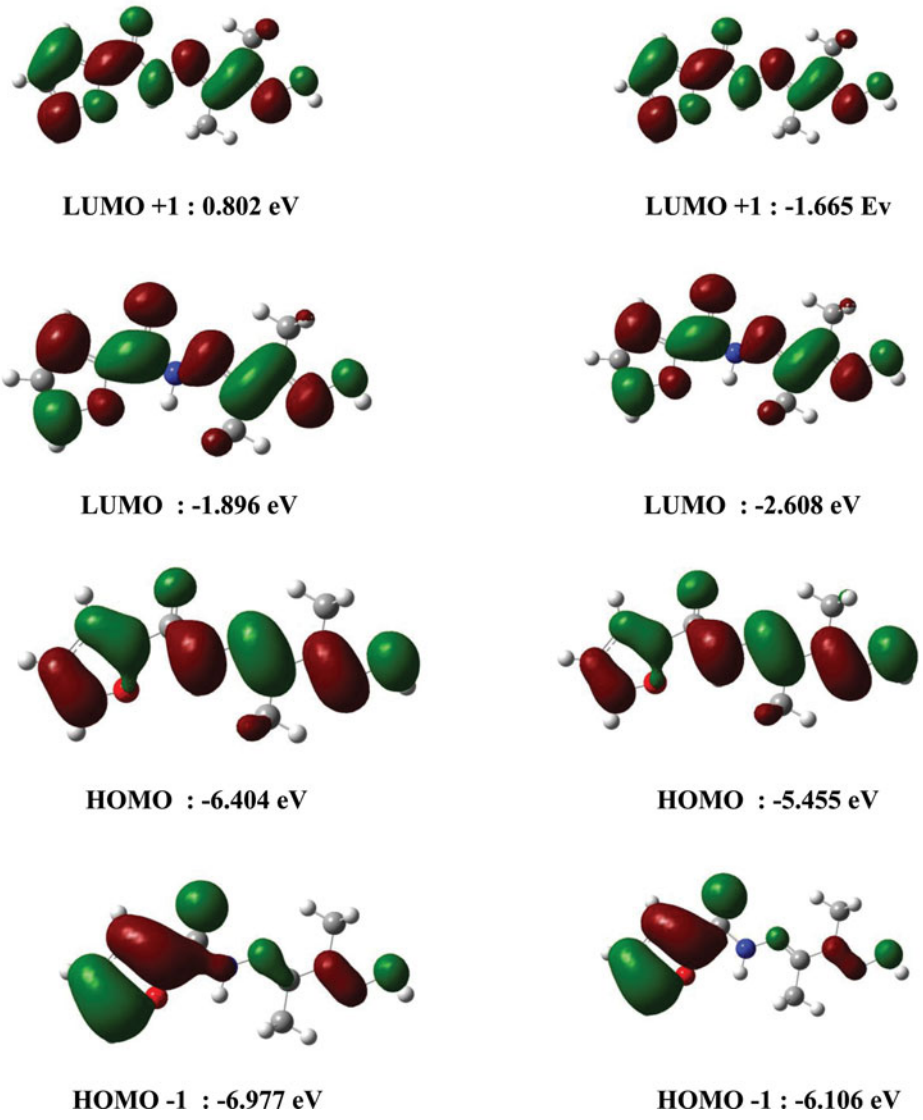


**Figure 5.** The atomic orbital compositions of the frontier molecular orbital for the title compound by B3LYP/6–311G(d, p) and PBEPBE/6–311G(d, p).

transfer interaction within the optimized molecule, and this gap is found to be 4.508 eV and 2.847 eV for methanol solvent with 4.507 eV and 2.848 eV for acetonitrile solvent by using B3LYP/6–311G(d, p) and PBEPBE/6–311G(d, p) basis sets, respectively. Besides these properties of the molecule, we have calculated ionization energy, electron affinity, electronegativity, chemical hardness and chemical softness of the molecule with DFT. The energy HOMO is sometimes considered as an approximation to the ionization energy while the energy LUMO is considered as an approximation to the electron affinity. The ionization energy ($I$) and electron affinity ($A$) can be obtained as $I = -E_{\mathrm{HOMO}}$ and $A = -E_{\mathrm{LUMO}}$. Electronegativity ($\chi$) can be calculated as follows: $\chi = (I + A)/2$. Chemical softness ($S$) is a property of molecule that measures the extent of chemical reactivity. It is the reciprocal of hardness $S = 1/2\eta$. It is defined as the reciprocal of chemical hardness ($\eta$) and $\eta = (I - A)/2$ [44]. The ionization energies of the molecule are 6.404 and 5.455 eV for B3LYP/6–311G(d, p) and PBEPBE/6–311G(d,

p) basis sets, respectively. The electron affinity of the molecule are 1.896 and 2.608 eV for B3LYP/6–311G(d, p) and PBEPBE/6–311G(d, p) basis sets, respectively. The electronegativity of the molecule are 4.150 and 4.031 eV for B3LYP/6–311G(d, p) and PBEPBE/6–311G(d, p) basis sets, respectively. The chemical hardness of the molecule are 2.254 and 1.423 eV for B3LYP/6–311G(d, p) and PBEPBE/6–311G(d, p) basis sets, respectively. The chemical softness of the molecule are 0.222 and 0.351 eV for B3LYP/6–311G(d, p) and PBEPBE/6–311G(d, p) basis sets, respectively.

## 4. Conclusion

In this study, we investigate X-ray structure, IR, UV, $^{1}$H NMR and $^{13}$C NMR spectra of the title compound. In addition to the experimental studies, most of the properties of the molecular structure have been calculated by using B3LYP/6–311G(d, p) and PBEPBE/6–311G(d, p) basis sets. Single crystal structure has been compared to the optimized molecular structure. It was noted that the experimental results belong to solid phase and theoretical calculations belong to gaseous phase. Despite the differences observed in the geometric parameters, the general agreement is good and the theoretical calculations support the solid state structures. However, it can be seen from the theoretical results that the B3LYP base function is more appropriate than the PBEPBE base function for the calculation of vibrational frequencies, chemical shift and molecular orbital analyses.

## Supplementary data

Crystallographic data for the structural analysis have been deposited with the Cambridge Crystallographic Data Centre, CCDC No 1058076. Copies of this information may be obtained free of charge from the Director, CCDC, 12 Union Road, Cambridge CB2 1EZ, UK (fax: +44–1223–336033; e-mail: deposit@ccdc.cam.ac.uk or www: http://www.ccdc.cam.ac.uk).

## Supplementary Information

Besides experimental studies, harmonic vibrational frequencies, $^{13}$C and $^{1}$H NMR, electrostatic potential map and thermodynamic parameters were calculated by using B3LYP/6–311G(d, p) and PBEPBE/6–311G(d, p). The results of harmonic vibrational frequencies are tabulated in S1. The theoretical $^{13}$C and $^{1}$H chemical shift values (with respect to TMS) of the title compound in DMSO solvent are tabulated in S2. The thermodynamic parameters can be seen from S3. Electrostatic potential map calculated by using B3LYP/6–311G(d, p) of the compound can be seen from S4.

## Acknowledgments

The authors wish to acknowledge the Faculty of Arts and Sciences, Ondokuz Mayis University, Turkey, for the use of the STOE IPDS-II diffractometer (purchased under Grant F.279 of the University Research Fund).

## References

[1] Al-Ne'aimi, M. M., & Al-Khuder, M. M. (2013). *Spectr. Acta Part: Mol.Bıo. Spec.*, *105*, 365.
[2] Armbruster, F., Klingebiel, U., & Noltemeyer, M. (2006). *Z. Naturforsch.*, *61b*, 225.
[3] Senturk, O. S., Sert, S., & Ozdemir, U. (2003). *Z. Naturforsch.*, *58b*, 1124.
[4] Amr, A.E.G.E., Mohamed, A. M., & Ibrahim, A. A. (2003). *Z. Naturforsch.*, *58b*, 861.

[5] Mohrle, H., & Keller, G. (2003). *Z. Naturforsch.*, *58b*, 885.
[6] Chakraborty, J. et al. (2006). *Z. Naturforsch.*, *61b*, 1209.
[7] Lozan, V. et al. (2003). *Z. Naturforsch.*, *58b*, 1152.
[8] Zeyrek, C. T., Elmali, A., & Elerman, Y. (2006). *Z. Naturforsch.*, *61b*, 237.
[9] Dey, D. K., Samanta, B., Lycka, A., & Dahlenburg, L. (2003). *Z. Naturforsch.*, *58b*, 336.
[10] Janiak, C., Lassahn, P. -G., & Lozan, V. (2006). *Macromol. Symp.*, *236*, 88.
[11] Katyal, M., & Dutt, Y. (1975). *Talanta*, *22*, 151.
[12] Mohan, M. M., Gupta, P., Chandra, L., & Jha, N. K. (1988). *Inorg. Chim. Acta*, *151*, 61.
[13] Sinh, R. B., & Jain, P. (1982). *Talanta*, *29*, 77.
[14] Molodykh, Zh. V., Buzykin, B. I., Bystrykn, N. N., & Kitaev, Y. P. (1978). *Khim. Farm. Zh.*, *11*, 37.
[15] Suez, I., Pehkonen, S. O., & Hoffmann, M. R. (1994). *Sci. Technol.*, *28*, 2080.
[16] Terra, L. H., Areias, A. M. C., Gaubeur, I., & Suez-Iha, M. E. V. (1999). *Spectr. Lett.*, *32*, 257.
[17] Sausa, G. D. et al. (2013). *Chem. Acta*, *86*, 201.
[18] Venkateswar Rao, P., Ashwini, K., & Ammani, S. (2007). *Bull. Chem. Soc. Ethiop.*, *21*, 63.
[19] Kumar, S., Singh, S. K., Vardhan, V., & Sharma, T. R. (2012). *Orient. J. Chem.*, *28*, 1837.
[20] Yaul, A. R., Dhande, V. V., & Aswar, A. S. (2010). *Rev. Roum. Chim.*, *55*, 537.
[21] Lei-Zhen, G., Jıng, X., Wie, W.. & Yin–Zhuang, Z. (2012). *Chinese J. Struct. Chem.*, *31*, 562.
[22] Babahan, I., Coban, E. P., & Bıyık, H. (2013). *Maejo Int. J. Sci. Technol.*, *7*, 26.
[23] Al-Ne'aimi, M. M., Al-Khuder, M. M., & Mohammed, S. J. (2012). *Raf. J. Sci.*, *23*, 51.
[24] Chaudhary, Dr. R., & Shelly, Dr. (2011). *Int. J. of Adv. Eng. Tecn.*, *2*, 100.
[25] El-Hendawy, A. M., Fayed, A. M., & Mostafa, M. R. (2011). *Trans. Met Chem.*, *36*, 352.
[26] Anupam, V., Pandeya, S. N., & Shweta, S. (2011). *Int. J. Res. Ayurveda Pharm.*, *2*, 1110.
[27] Assayehegn, E. "Synthesis and structural studies on metal complex based on multidentate ligand derived from salicylaldehyd and resdiacetophenone-dihydrazone", Addis Ababa universıty scholl of graduate studies department of chemistry graduate program, August, 2007.
[28] Kumar, M., & Saxena, P. N. (2012). *Ori. J. Chem.*, *28*, 1927.
[29] Stoe&Cie (2002). *X-AREA(Version 1.18) and X-RED32 (Version 1.04)*, Stoe&Cie: Darmstadt, Germany.
[30] Sheldrick, G. M. (1997). SHELXS 97 and SHELXL 97, University of Göttingen: Germany.
[31] Sheldrick, G. M. (2013). SHELXL2013, University of Göttingen: Germany.
[32] Farrugia, L. J. (1998). ORTEP-3, University of Glasgow: UK.
[33] Becke, A. D. (1993). *J. Chem. Phys.*, *98*, 5648.
[34] Lee, C., Yang, W., & Parr, R. G. (1988). *Phys. Rev.*, *B37*, 785.
[35] Ditchfield, R. (1972). *J. Chem. Phys.*, *56*, 5688.
[36] Wolinski, K., Hinton, J. F., & Pulay, P. (1990). *J. Am. Chem. Soc.*, *112*, 8251.
[37] Frish, A., Nielseni, A. B., & Holder, A. J. (2001). Gaussview user manual, Gaussian Inc.: Pittsburg, PA.
[38] Frisch, M. J. et al. (2004). Gaussian 03, Gaussian, Inc.: Wallingford, CT.
[39] Hökelek, T., Batı, H., Bekdemir, Y., & Kütük, H. (2001). *Acta Cryst.*, *E57*, o663.
[40] Zülfikaroğlu, A., Yüksektepe, Ç., Batı, H., Çalışkan, N., & Büyükgüngör, O. (2009). *J. Struct. Chem.*, *50*, 1166.
[41] Okabe, N., Nakamura, T., & Fukuda, H. (1993). *Acta Cryst.*, *C49*, 1678.
[42] Saracoğlu, H. et al. (2004). *Acta Cryst.*, *E60*, o1307.
[43] Zülfikaroğlu, A., Yüksektepe, Ç., Batı, H., & Çalışkan, N. (2010). *R. J. Coord. Chem.*, *36*, 124.
[44] Chermette, H. (1999). *J. Comput. Chem.*, *20*, 129.